

The Antennae Ultraluminous X-Ray Source, X-37, Is A Background Quasar

D.M. Clark ¹, M.H. Christopher ², S.S. Eikenberry ¹, B.R. Brandl ³, J.C. Wilson ⁴, J.C. Carson ⁵, C.P. Henderson ⁶, T. L. Hayward ⁷, D.J. Barry ⁶, A.F. Ptak ⁸, E.J.M. Colbert ⁸

ABSTRACT

In this paper we report that a bright, X-ray source in the Antennae galaxies (NGC 4038/9), previously identified as an ultra-luminous X-ray source, is in fact a background quasar. We identify an isolated infrared and optical counterpart within $0.3 \pm 0''.5$ the X-ray source X-37. After acquiring an optical spectrum of its counterpart, we use the narrow [OIII] and broad H α emission lines to identify X-37 as a quasar at a redshift of $z=0.26$. Through a U , V , and K_s photometric analysis, we demonstrate that most of the observable light along this line of sight is from the quasar. We discuss the implications of this discovery and the importance of acquiring spectra for optical and IR counterparts to ULXs.

Subject headings: quasars: general – galaxies: starburst – X-rays: galaxies

1. Introduction

Ultraluminous X-ray sources (ULX) are typically defined as point sources with X-ray luminosities $> 10^{39}$ ergs s⁻¹. *Einstein* (Long & van Speybroeck 1983; Helfand 1984; Fabbiano 1989) and *ROSAT* (Roberts & Warwick 2000; Colbert & Ptak 2002) observations revealed

¹Department of Astronomy, University of Florida, Gainesville, FL 32611; dmclark@astro.ufl.edu

²Caltech, Department of Astronomy, 105-24, Pasadena, CA 91125.

³Leiden Observatory, 2300 RA Leiden, Netherlands.

⁴Department of Astronomy, P.O Box 3818, University of Virginia, Charlottesville, VA 22903.

⁵JPL, Earth & Space Science, Pasadena, CA 91109.

⁶Astronomy Department, Cornell University, Ithaca, NY 14853.

⁷Gemini Observatory, AURA/Casilla 603, La Serena, Chile

⁸Department of Physics and Astronomy, Johns Hopkins University, 3400 North Charles St., Baltimore, MD 21218.

many of these objects in nearby galaxies. Recent *Chandra* observations indicate the Antennae (NGC 4038/4039) contain 9 ULXs (Zezas, et al. 2002a, assuming here and hence forth $H_0 = 75 \text{ km s}^{-1} \text{ Mpc}^{-1}$), the largest number discovered so far in a single galaxy (Fabbiano, et al. 2003).

One X-ray source in the Antennae that has received considerable attention in the recent literature is X-37, as designated by Zezas, et al. (2002a). At the distance to these interacting galaxies (19.3 Mpc) it would have an X-ray luminosity, $L_x = 4.5 \times 10^{39} \text{ ergs s}^{-1}$, making it a ULX. A previous attempt to match X-ray positions directly to *HST* positions indicated that this object has a significant ($> 1''0$) offset from a nearby optical source (Zezas, et al. 2002b). This spawned discussions of whether this is a runaway X-ray binary escaping from its parent cluster (Zezas, et al. 2002b; Miller, et al. 2004a; Fabbiano 2004). But, matching X-ray positions directly to the optical is difficult due to the crowded *HST* field and image rotation.

In Clark, et al. (2005) (henceforth Paper 1) we demonstrated that the infrared (IR) is a powerful method for finding counterparts to X-ray sources. This wavelength regime has similar dust penetrating properties to X-rays, facilitating counterpart identification. In a subsequent paper we match X-ray and optical *HST* positions with high precision by using the IR frame tie as a go-between (Clark, et al. 2005, in preparation; henceforth Paper 2). Here we use X-37 to demonstrate the success of our method and show the importance of obtaining follow-up spectra of counterparts to ULX candidates. §2 describes our spectroscopic observations and briefly discusses our analysis of the IR and optical images. We summarize our results and present the implications of our discovery in §3.

2. Observations and Data Analysis

2.1. Infrared and Optical Images

Our analysis of the counterpart to X-37 is based in part on IR *J* ($1.25 \mu\text{m}$) and *K_s* ($2.15 \mu\text{m}$) band images of the Antennae. These images were first analyzed by Brandl, et al. (2005), who reported the details of the data reduction. In summary, we acquired 20 minute total exposures in each filter using the Wide-field InfraRed Camera (WIRC) on the Palomar 5-m telescope during the night of March 22nd, 2002.

In Paper 1, we made a frame tie between the IR and X-ray using IR counterparts to compensate for the poor astrometric accuracy of *Chandra* ($\sim 1''5$). We matched 7 IR sources from the WIRC images with *Chandra* X-ray point sources. Using a least squares fit of a linear matching function we tied *Chandra* R.A. and Dec. to WIRC x,y pixel positions. The RMS

positional uncertainty is $\sim 0''.5$.

With the astrometric frame tie in place, we identified a bright, $K_s = 16.2$ mag source $0.3 \pm 0''.5$ from the X-ray position of X-37 (see Figure 1). Note that this contradicts previous reports of a significant offset between X-37 and the star cluster candidate, and independently eliminates any need for the hypothesis that this X-ray source is a runaway X-ray binary (Zezas & Fabbiano 2002; see also Miller et al. 2004a; Fabbiano et al. 2003).

We also base this study on work done in Paper 2 where we studied optical counterparts to X-ray sources in the Antennae. We obtained archival *HST* images (Whitmore, et al. 1999) in the following filters: F336W(*U*), F439W(*B*), F555W(*V*), and F814(*I*). Tying *Chandra* X-ray coordinates to *HST* positions is nontrivial due to image rotation and the crowded field in the *HST* images. Instead, we used our excellent frame tie between the IR and X-ray as an intermediate step. We used the same basic procedure as that used in Clark, et al. (2005). Using this astrometric frame tie, we found an optical source $0.6 \pm 0''.6$ from the X-ray position of X-37 (Figure 1) — again, an insignificant offset.

2.2. Spectroscopy

We acquired an optical spectrum of X-37 on March 7, 2003, using the Low Resolution Imaging Spectrograph (Oke, et al. 1995, LRIS) on Keck I. We observed this source in two separate slitmasks with a $400 \text{ lines mm}^{-1}$ grating and blaze wavelength of 8500 \AA , yielding a total wavelength coverage on the red side of $5600\text{-}9400 \text{ \AA}$. Seeing throughout the observations was $\sim 0''.8$. We observed X-37 for a total of 6000 seconds between the two masks with typical single exposure times of 600 seconds.

We reduced the spectrum with a combination of standard IRAF procedures and IDL code using the NeAr arc-lamp spectrum for wavelength calibration. We used the standard star Feige 67 to flux calibrate the spectrum.

We extracted spectra of the X-37 counterpart from each individual exposure in a $1''.8$ (approximately 2 FWHM) region centered on the emission peak. A background spectrum extracted from a region $2''$ removed from the counterpart was sufficient for removing the night sky lines. We point out the blended lines, $\text{H}\alpha$ /[NII] at $\sim 6600 \text{ \AA}$ and the [SII] pair at $\sim 6750 \text{ \AA}$, observed at the redshift of the Antennae (Figure 2). These spectral features are at approximately the same levels in the on-source and background spectra, suggesting that they are likely diffuse emission from the Antennae and not associated with X-37.

Noting the broad emission lines characteristic of a quasar we looked for other spectral

features to confirm this classification. The realization that the broad line at 8296 Å was red-shifted H α prompted a search for additional lines generally associated with quasars. We noted a plethora of such identifiers including the non-restframe wavelengths of H β at 6148 Å, [OI] at 7965 Å, [NII] at 8320 Å, and [SII] at 8510 Å. This corroborated our conclusion that X-37 is a quasar.

Using the observed, narrow [OIII] lines at 6270.45 Å and 6330.94 Å, we measured a redshift of $z=0.26$. At the redshift to this quasar, X-37 would now have an X-ray luminosity of $L_x = 1.4 \times 10^{43}$ ergs s $^{-1}$. As we show in Table 1, this luminosity is typical of the X-ray luminosity for quasars at a similar distance (Schartel, et al. 1996).

2.3. Photometry

To investigate how much of the continuum flux could be due to the quasar, we compared the photometric properties of this source to that of other quasars at X-37’s redshift of $z=0.26$. We chose U and V -band photometry from the *HST* images and K_s -band photometry from the WIRC images. This choice in filters covers the full wavelength range used in our studies of the Antennae (Clark, et al. 2005, in preparation). The full-width at half-maximum (FWHM) in U , V , and K_s are 0’24, 0’18 and 0’9, respectively. Defining the photometric aperture as $\sim 3\sigma$ of the Gaussian point spread function (PSF) width, the aperture radii are 3-pixels in U , 2.5-pixels in V , and 5-pixels in K_s .

Subtracting sky background flux is especially difficult in the Antennae considering the bright, crowded background in these galaxies. To compensate for this difficulty, we chose to measure the mean and median sky background flux in two separate annuli between $\sim 6 - 10\sigma$ of the PSF. Being an isolated source, we did not have to compensate for crowded conditions in the field around the X-37 counterpart. Multiplying the mean and median sky background by the area of the central aperture and then subtracting this from the central aperture yielded four separate flux measurements for the source. We then averaged these four values to give us the source flux. When computing errors, we considered variations in the sky background, σ_{sky} , and Poisson noise, σ_{adu} . To calculate σ_{sky} we found the standard deviation of the four flux values for each source. Dividing the mean source flux by the instruments gain and then taking the square root of these, we found σ_{adu} . The known gain for WIRC is 2 e $^{-1}$ /DN (Wilson, et al. 2003), while Whitmore, et al. (1999) use a gain of 7 e $^{-1}$ /DN for *HST*. Both σ_{sky} and σ_{adu} were added in quadrature to yield a total error in flux, σ_{flux} .

We used a bright, 2MASS star to convert K_s flux into a magnitude. We derived *HST* magnitudes using zero points listed in Table 28.1 of the *HST* Data Handbook (Voit 1997).

Applying color transformations defined in Holtzman, et al. (1995), we converted *HST* magnitudes to Johnson *U* and *V*. We expressed errors in magnitude, σ_m , as σ_{flux} divided by the mean flux. In the case of *U* and *V*, σ_m consists of the additional errors in the zeropoint and color transformations, all of which were added in quadrature.

2.3.1. Absolute Magnitudes

We next converted these photometric measurements to reddening-corrected absolute magnitudes. At the redshift of X-37, the distance modulus is 40.1 mag. We derived reddening in *V*, $A_V = 1.3$ mag, using the X-ray derived column density, N_H , listed in Table 5 of Zezas, et al. (2002a) and the relationship $A_V = 5 \times 10^{-22} \text{ cm}^{-2} N_H$. We used the N_H value provided by the power-law spectral fits of Zezas, et al. (2002a). These authors computed N_H assuming the absorption is at zero redshift. This should not be a problem for us since the broad absorption lines observed in the X-37 spectrum suggest there is little extinction along the line of sight to it.

To find reddening in other filters, we used the extinction law defined in Cardelli, Clayton, & Mathis (1989, CCM). We also computed separate reddenings in each filter using the Rieke-Lebofsky (RL) Law (Rieke & Lebofsky 1985). We then expressed errors in reddening, σ_A , as the difference in A_U , A_V and A_{K_s} derived from each law. Adding σ_A and σ_m in quadrature, we computed a total error in absolute magnitude.

In Table 1, we compare the absolute magnitudes, M_U , M_V , and M_{K_s} , of the X-37 counterpart to typical magnitudes for quasars at a similar distance. We obtained M_U and M_V from the Sloan Digital Sky Survey (SDSS) quasar catalog (Schneider, et al. 2003) for 33 quasars at a redshift of 0.26. Using color transformations listed in Fukugita, et al. (1996), we converted SDSS magnitudes to the Johnson photometric system. We used the catalog described in Barkhouse & Hall (2001) to derive M_{K_s} for 17 quasars at a redshift of 0.26. Considering the absolute magnitude of X-37 in the *U*, *V* and *K_s* bands falls within the range of catalog quasar magnitudes, X-37 has the luminosity of a typical quasar.

3. Discussion

The identification of X-37 with a background quasar further demonstrates the importance of spectroscopic followup for the study of ULX sources. While the overabundance of such sources near galaxies clearly demonstrates that a physical connection does exist for many ULX sources as a population (e.g. Colbert & Ptak 2002), the strong possibility of back-

ground quasar contamination makes such identification for any particular source perilous (see also Gutiérrez & López-Corredoira 2005).

A specific example involving X-37 is the recent work of Miller, et al. (2004b). In their Figure 2, Miller, et al. (2004b) compare the black hole mass to inner disk temperature for both ULX sources and “standard” stellar-mass black holes, finding that the ULX sources have cooler disk temperatures. They use this to conclude that ULX are likely to be powered by accretion onto Intermediate-Mass Black Holes (IMBH). While some of the sources in this diagram are almost certainly ULXs (i.e. NGC 1313 X-1 and NGC 1313 X-2), and thus possible IMBH, it is somewhat surprising to note that the “ULX” X-37 is grouped with these sources in the diagram – despite the fact that its actual black hole mass is at least 4 orders of magnitude higher than assumed by Miller, et al. (2004b). Thus, X-37 illustrates the importance of follow-up spectroscopic confirmation of ULXs, and sounds a cautionary note regarding conclusions based on observations without such confirmation.

The authors are especially grateful to Fred Hamann and Vicki Sarajedini for examining our spectra and helping identify this unusual source as a quasar. We also thank J. Houck for his support of the WIRC instrument project. WIRC was made possible by support from NSF (NSF-AST0328522), the Norris Foundation, and Cornell University. SSE and DMC are supported in part by an NSF CAREER award (NSF-9983830).

REFERENCES

- Antonucci, R. 1993, *ARA&A*, 31, 473
- Barkhouse, W.A. & Hall, P.B. 2001, *AJ*, 121, 2843
- Brandl, B.R., et al. 2005, *ApJ*, submitted
- Cardelli, J.A., Clayton, G.C., & Mathis, J.S. 1989, *ApJ*, 345, 245
- Clark, D.M., et al. 2005, *ApJ*, submitted
- Colbert, E.J.M., & Ptak, A.F. 2002, *ApJS*, 143, 25
- Fabbiano, G. 2004, *RevMexAA*, 20, 46
- Fabbiano, G., Zezas, A., King, A.R., Ponman, T.J., Rots, A., & Schweizer, F. 2003, *ApJ*, 584, 5
- Fabbiano, G., Zezas, A., & Murray, S.S. 2001, *ApJ*, 554, 1035
- Fabbiano, G. 1989, *ARA&A*, 27, 87
- Fukugita, M., Ichikawa, T., Gunn, J.E., Doi, M., Shimasaku, K., Schneider, D.P. 1996, *AJ*, 111, 1748
- Gutiérrez, C.M., & López-Corredoira, M. 2005, *ApJ*, 622, L89
- Helfand, D.J. 1984, *PASP*, 96, 913
- Holtzman, J.A., et al. 1995, *PASP*, 107, 1065
- Long, K.S., & van Speybroeck, L.P. 1983, in *Accretion-Driven X-Ray Sources*, ed. W.H.G. Lewin, & E.P.J. van den Heuvel (Cambridge: Cambridge Univ. Press) 117
- Miller, J.M., Zezas, A., Fabbiano, G., & Schweizer, F. 2004a, *ApJ*, 609, 728.
- Miller, J.M., Fabian, A.C., & Miller, M.C. 2004b, *ApJ*, 614, L117
- Miller, J.M., Fabbiano, G., Miller, M.C., & Fabian, A.C. 2003, *ApJ*, 585, L37
- Oke, J.B., et al. 1995, *PASP*, 107, 375
- Rieke, G.H., & Lebofsky, M.J. 1985, *ApJ*, 288, 618
- Roberts, T.P., & Warwick, R.S. 2000, *MNRAS*, 315, 98

Schartel, N., Walter, R., Fink, H.H., & Trümper, J. 1996, *A&A*, 307, 33

Schneider, D.P., et al. 2003, *AJ*, 126, 2579

Voit, M. 1997, *HST Data Handbook* (Baltimore: STScI)

Whitmore, B.C., Zhang, Q., Leitherer, C., Fall, S.M., Schweizer, F., & Miller, B.W. 1999, *AJ*, 118, 1551

Wilson, J.C., et al. 2003, *SPIE*, 4841, 451

Zezas, A.L., Fabbiano, G., Rots, A.H., & Murray, S.S. 2002a, *ApJS*, 142, 239

Zezas, A.L., Fabbiano, G., Rots, A.H., & Murray, S.S. 2002b, *ApJ*, 577, 710

Table 1. Absolute Magnitude Comparison to Quasars at $z \approx 0.26$

Filter	Observed Magnitudes ¹	Typical Catalog Range
U	-20.9 ± 0.2	$-23.9 - -20.8$
V	-20.4 ± 0.2	$-23.4 - -21.0$
K_s	-24.1 ± 0.1	$-25.6 - -23.8$
$\log(L_x)$	43.1	43.7 – 44.1

¹Absolute magnitudes include uncertainties in each value. Catalog values were taken from separate sources: U and V from Schneider, et al. (2003), K_s from Barkhouse & Hall (2001), and L_x from Schartel, et al. (1996).

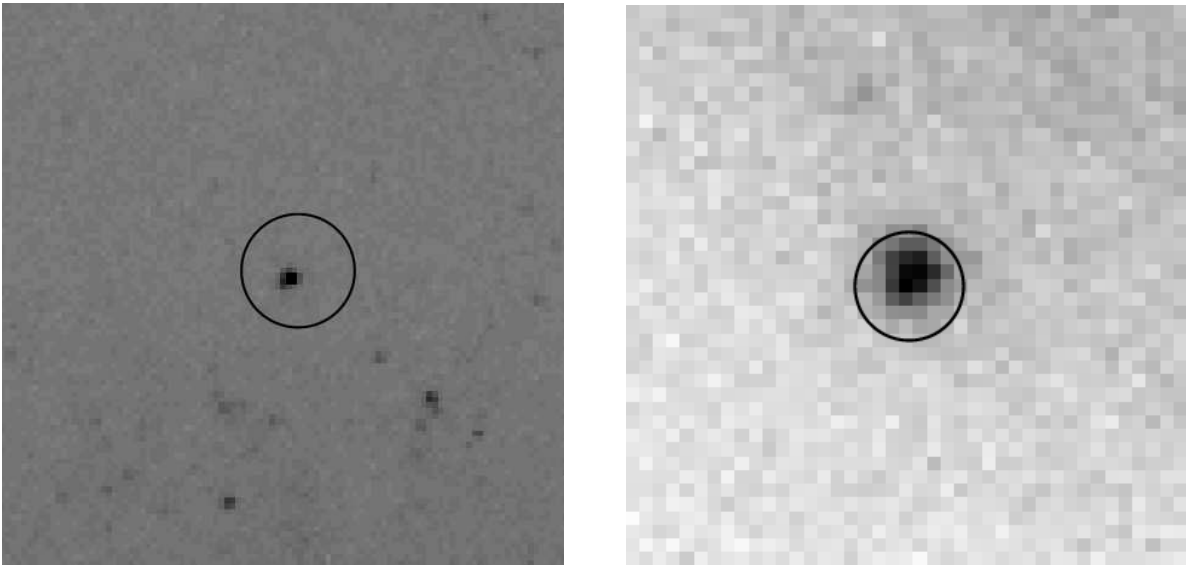


Fig. 1.— U band image (left) and K_s band image (right) showing a 1-arcsecond positional error circle centered on the X-ray source, X-37. Notice the bright source well within this circle.

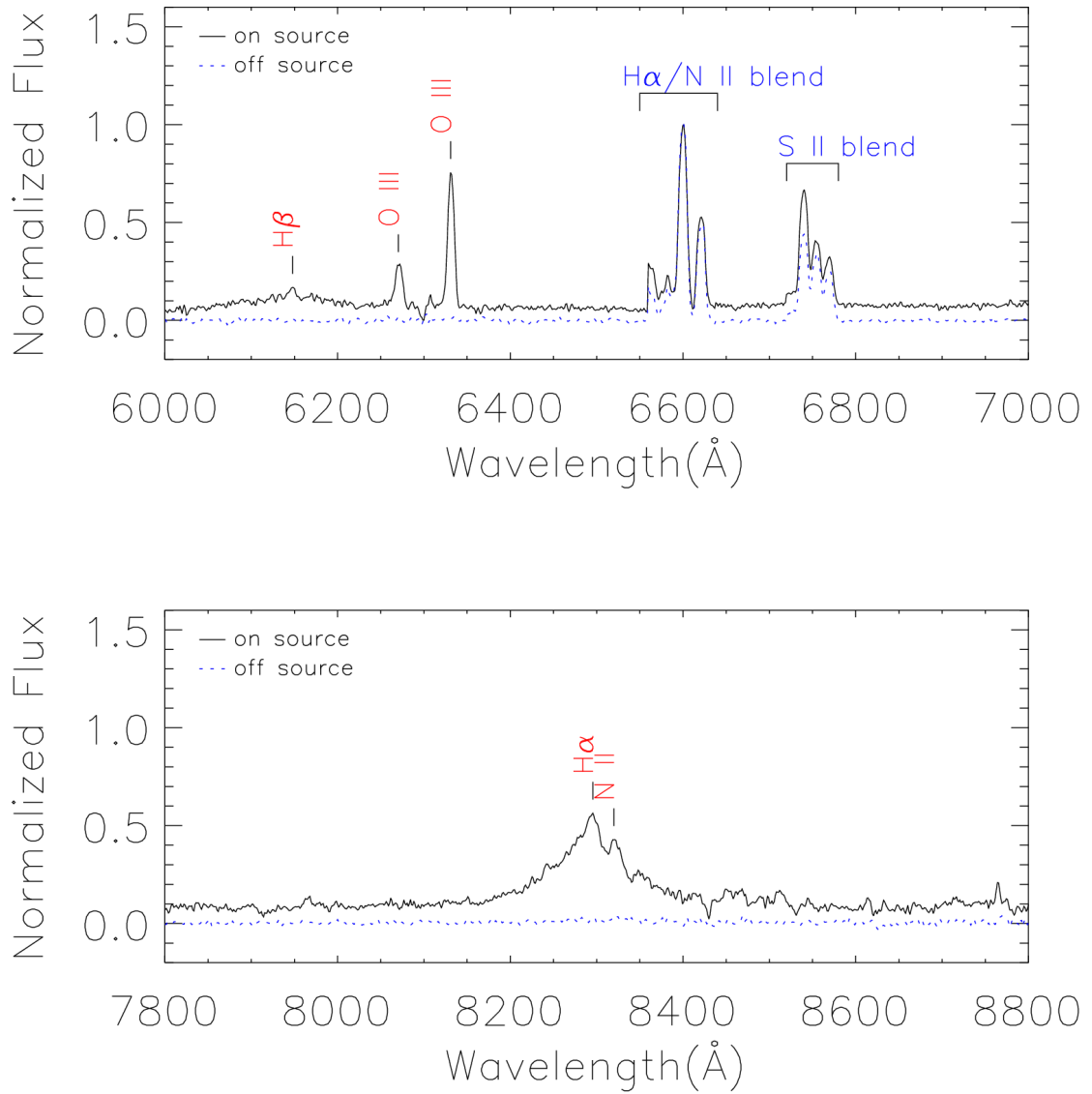


Fig. 2.— X-37 spectrum. Red text denotes quasar lines, blue text denotes lines from the Antennae background emission.